

Simulated Annealing Based Heuristic for Multiple Agile Satellites Scheduling under Cloud Coverage Uncertainty

Chao Han, Yi Gu, Guohua Wu, *Member, IEEE*, and Xinwei Wang

Abstract—Agile satellites are the new generation of Earth observation satellites (EOSs) with stronger attitude maneuvering capability. Since optical remote sensing instruments equipped on satellites cannot see through the cloud, the cloud coverage has a significant influence on the satellite observation missions. We are the first to address multiple agile EOSs scheduling problem under cloud coverage uncertainty where the objective aims to maximize the entire observation profit. The chance constraint programming model is adopted to describe the uncertainty initially, and the observation profit under cloud coverage uncertainty is then calculated via a sample approximation method. Subsequently, an improved simulated annealing-based heuristic combining a fast insertion strategy is proposed for large-scale observation missions. Finally, extensive experiments are conducted to verify the effectiveness and efficiency of the proposed method. Experimental results show that the improved simulated annealing-based heuristic outperforms other algorithms for the multiple AEOSs scheduling problem under cloud coverage uncertainty, which verifies the efficiency and effectiveness of the proposed algorithm.

Index Terms—agile Earth observation satellite, chance constraint programming, cloud coverage uncertainty, sample approximation, simulated annealing

I. INTRODUCTION

Earth observation satellite (EOS), which serves as a space platform orbiting the Earth, utilizes remote sensors to collect images of targets on the Earth surface [1]. With the advantage of space locations, the EOS has been applied to many fields, such as resource exploration, weather prediction and disaster alerts [2].

Agile Earth observation satellites (AEOSs) are the new generation of EOSs. Compared to conventional EOSs (CEOSs), AEOSs have considerable improvement in attitude maneuverability. Fig. 1 shows different observation conditions for three candidate targets between CEOS and AEOS, in which visible time window (VTW) is the time window during which the target is visible for a satellite and observation window (OW) denotes the actual observation time window. Detailed calculation procedure of VTWs can be found in [3], [4].

Chao Han and Yi Gu are with the School of Astronautics, Beihang University, Beijing, 100191, China (e-mail: hanchao@buaa.edu.cn; guyi_buaa@buaa.edu.cn)

Guohua Wu and Xinwei Wang are with School of Traffic and Transportation Engineering, Central South University, Changsha, 410000, China (e-mail: guohuawu@csu.edu.cn; xinwei.wang.china@gmail.com) (*Corresponding author*: Xinwei Wang)

This work has been submitted to the IEEE for possible publication. Copyright may be transferred without notice, after which this version may no longer be accessible.

With the attitude maneuvering ability of roll axis, CEOS can only perform observation missions when it is right above targets on the Earth surface. As shown in Fig. 1, the conflict between targets 1 and 2 is therefore inevitable for CEOS owing to the time overlapping. However, both two targets can be observed by single AEOS with stronger observation capacity arising from the maneuverability of pitch axis. Possessing three degrees of freedom (roll, pitch and yaw axes), AEOS is able to observe targets for longer periods [5], which better satisfies users' requirements.

Despite the advantages of AEOS compared to CEOS, the AEOS mission scheduling is more difficult. Through the adjustment of pitch axis, AEOS could access longer VTW for each target, generally exceeding the required observation time [5]. Therefore, it is necessary to determine the observation start time for each target. In Fig. 1, the optional range of the observation start time OTS_1 for target 1 varies in time period $[VTS_1, VTE_1 - ot_1]$, greatly increasing the scheduling complexity. Meanwhile, the attitude transformation time constraint between two adjacent targets should be taken into consideration; the AEOS has to accomplish the roll and pitch attitude transformation between targets 1 and 2. The energy consumption in both attitude maneuvering process and observation operation should also be considered. Notice that the attitude of AEOS for observation mission depends on the observation start time, which consequently determines the transition time between two adjacent targets. Hence, the selection of observation start time results in the coupling of feasible transition time constraints and energy constraints. Given all above characteristics, Lematre *et al.* [6] indicated that the AEOS scheduling problem, although simplified, is NP-hard.

A number of cross-sectional studies contributed to CEOS scheduling problems. Gabrel *et al.* [7], [8] presented a graph-theoretic model and derived exact and inexact algorithms. Wolfe and Sorensen [9] introduced the window-constrained-packing model for EOS scheduling. Benoist and Rottembourg [10] provided the upper bound of the observation profit optimization, using the generalized traveling salesman problem with time windows. Lin *et al.* [11] proposed a Lagrangian relaxation method to solve the daily imaging scheduling of single CEOS. Marinelli *et al.* [12] formulated the problem as a time-indexed integer programming. Wu *et al.* [13], [14], [15] has taken the mission clustering strategy into satellite scheduling problem and proposed several efficient algorithms. Wang *et al.* [16] adopted the flow formulation to describe the

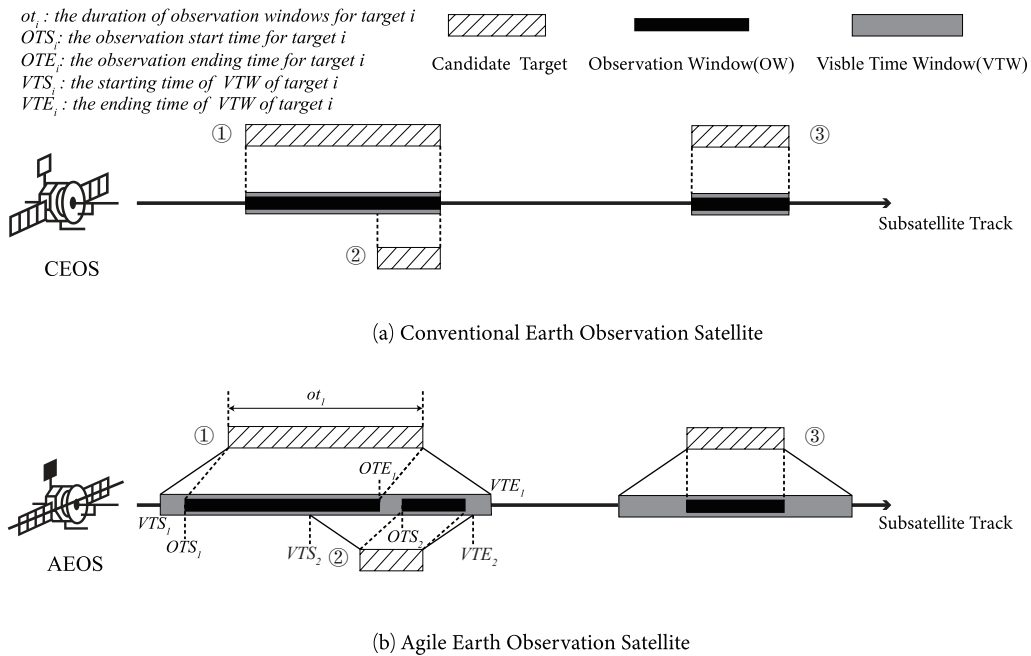


Fig. 1. Comparison between CEOS and AEOS.

fixed interval scheduling of multiple CEOSs. Considering the feature of limited resource capacities, Chen *et al.* [2] proposed a mixed integer linear programming for multi-satellite scheduling. Hu *et al.* [17] designed a branch-and-price algorithm for CEOSs constellation imaging and downloading integrated scheduling problem.

Meanwhile, enormous research about agile satellite scheduling has been conducted [18]. The mission management problem of AEOS was first set out and analyzed by Lematre *et al.* [6]. Beaumet *et al.* [19], Liu *et al.* [20] and She *et al.* [21] studied the scheduling problem of agile satellite autonomous mission planning. Wang *et al.* [22], [23] connected the theory of complex networks with AEOS redundant targets scheduling problem, and proposed a fast approximate scheduling algorithm. A metaheuristic based on large neighborhood search method was introduced to solve the time-dependent scheduling problem in [1], [5]. Cho *et al.* [24] formulated a two-step linear programming model for mission planning of satellite constellation. Li *et al.* [25] proposed a preference-based evolutionary algorithm in the multi-objective optimization of agile satellite mission planning. Du *et al.* [26] introduced a novel algorithm for area targets observation in which the drift angle constraint was considered. Peng *et al.* [27] proposed an exact algorithm to solve single AEOS scheduling problem considering time-dependent profits, where the profit of a target depends on the observation start time.

In practical satellite scheduling, the uncertainty, which originates from the change of mission priority, weather conditions and satellite resource status, is inevitable. Considerable researchers have studied the scheduling problem for both CEOS and AEOS, in which the uncertainty derived from dynamic missions and emergency responses have been considered [28], [29], [30], [31], [32]. On account of the widespread application

of optical sensors on the EOS, the observation mission is extremely influenced by the uncertainty of cloud coverage [33], [34]. It is reported that around 35% of the images acquired by the Landsat-7 sensors are blocked by cloud [35]. He *et al.* [36] also reported that about 60% current observations were useless owing to the cloud coverage, which demonstrated the significance considering cloud coverage in satellite scheduling. However, limited attention for EOS scheduling considering the cloud coverage is obtained. Liao *et al.* [37] formulated a stochastic integer programming model to represent the influence of cloud coverage. Wang *et al.* [38] employed a chance constrained programming (CCP) model to describe the stochasticity of cloud, and presented a branch-and-cut method to solve the problem. Utilizing scenarios representing the uncertainty of cloud coverage, Valicka *et al.* [39] introduced novel stochastic mixed integer programming models with the objective of maximizing collection quality when cloud cover uncertainty was considered. Wang *et al.* [40] further demonstrated the efficiency of the proposed exact and heuristic algorithm in the scheduling of multiple CEOSs under cloud coverage uncertainty. Besides, Wang *et al.* [41] developed an expectation model and a sample average approximation model, and comparative experiments have been conducted. A two-phased scheduling framework, taking advantage of hypothetical real-time cloud information, was associated to the AEOS scheduling in [42]. Unfortunately, the cloud coverage is always changing, which is quite difficult to be exactly predicted [43].

Several drawbacks still exist for the reviewed papers. First, despite extensive research of AEOS scheduling, few study has taken the uncertainty of cloud coverage into consideration, especially for the multi-AEOS scheduling problem. Second, current research about CEOS scheduling cannot be readily applied to AEOS uncertain scheduling, since the mathematical

model of CEOS scheduling has difficulty transforming into AEOS model. Moreover, the algorithms proposed for CEOS scheduling with uncertainty are not suitable owing to the enhanced attitude maneuverability of AEOS.

Motivated by the huge impact of the cloud coverage and the lack of corresponding AEOS scheduling research, we therefore address the multi-AEOS scheduling problem considering energy and memory constraints under cloud coverage uncertainty. The CCP model [44] is adopted to describe the uncertainty of cloud coverage, and the observation profit is then calculated via the sample approximation method. With respect to the characteristics of agile satellites, an optimization subproblem, solved by a sequential quadratic programming (SQP) method, is established to determine actual observation time windows. To solve the master optimization problem of maximizing the entire observation profit under uncertainty, an improved simulated annealing (ISA) based heuristic is developed, in which a fast insertion strategy plays an important role in arranging missions. Afterwards, we conduct extensive experiments to verify the effectiveness and efficiency of the proposed algorithm in solving multi-AEOS scheduling problem under cloud coverage uncertainty.

The contributions of this study are therefore summarized as follows:

- The multiple AEOSs scheduling problem considering energy and memory constraints under cloud coverage uncertainty is addressed in this work. The introduced uncertainties are mathematically represented with CCP and a sample approximation method.
- Utilizing the concept of time slack, an optimization subproblem of determining the observation start time is established, and we then propose a SQP based fast insertion algorithm, which plays a significant role to ensure efficient update of the scheduling solution.
- In order to effectively and efficiently solve the uncertain AEOSs scheduling problem, we propose an ISA based heuristic consisting of two stages: an initial solution is constructed using the selection rules of targets and resources at the first stage; and in the second stage, the ISA combining with the fast insertion algorithm is utilized to iteratively update the scheduling solution. Extensive experiments are conducted to demonstrate the superior performance of our proposed algorithm.

The remainder of this paper is organized as follows. In Section II, necessary definitions and problem descriptions are provided, and the CCP model is established. Section III introduces the sample approximation method to calculate the observation profit, defines the optimization subproblem of determining the start time of OW and proposes an ISA based heuristic. A series of experimental results are reported in Section IV. We summarize our work and point out future directions in the last section.

II. PROBLEM STATEMENT

In this section, the deterministic multi-AEOS scheduling problem is introduced at first, followed by the uncertain model considering cloud coverage uncertainty.

A. Deterministic AEOS scheduling

Based on the relative size between ground targets and the view horizon of satellite sensors, the observation objects can be divided into point targets and area targets in EOS scheduling. The area target can be decomposed into multiple point targets, therefore, we only consider the point targets in this study. Different satellite orbits are viewed as different orbital resources. The following assumptions and simplifications are further provided:

- 1) Each satellite conducts at most one observation mission in one time;
- 2) Each target cannot be observed more than once.
- 3) The attitude transformation time, energy and memory consumption are taken into consideration.
- 4) The process of data download is not considered.

TABLE I
NOTATIONS.

Target	
A	Set of observation targets, $A = \{1, \dots, A \}$ and $ A $ is the target set size
i, j	Target index, $i, j \in A \cup \{0, A + 1\}$, in which $0, A + 1$ are dummy targets
ot_i	The observation duration of target i , $i \in A$
ω_i	Observation profit of target i , $i \in A$
Orbit	
O	Set of orbits, $O = \{1, \dots, O \}$ and $ O $ is the orbit set size
k	Orbit index, $k \in O$
M_k, E_k	Memory and energy capacity on orbit k , $k \in O$
m_k, e_k	Memory and energy consumption for unit time of observation on orbit k
e'_k	Energy consumption for each unit angle of attitude transformation on orbit k
Decision variables	
x_{ik}	Binary decision variable. $x_{ik} = 1$ if target i is scheduled to be observed on orbit k , otherwise $x_{ik} = 0$, $i \in A, k \in O$
TP_{ik}	Continuous decision variable within $[0, 1]$. TP_{ik} is associated to the observation start time for target i on orbit k , $i \in A, k \in O$
Constraint parameters	
b_{ik}	$b_{ik} = 1$ if orbit k is available for the observation of target i , otherwise $b_{ik} = 0$, $i \in A, k \in O$
$[OTS_{ik}, OTE_{ik}]$	Observation time window of target i on orbit k , $i \in A, k \in O$
$[VTS_{ik}, VTE_{ik}]$	Visible time window of target i on orbit k , $i \in A, k \in O$
$Trans(i, j, k)$	Attitude transformation time between targets i and j on orbit k , $i, j \in A, k \in O$
se_{ij}^k	Energy consumption in the transformation from i to j on orbit k . $se_{ij}^k = 0$ if j is a dummy target, $i \in A, j \in A \cup \{ A + 1\}$, $k \in O$
λ_{ik}	Binary stochastic parameter, $\lambda_{ik} = 1$ denotes that target i is successfully observed on orbit k , and $\lambda_{ik} = 0$ otherwise
p_{ik}	Probability that target i will be successfully observed on orbit k , $i \in A, k \in O$
W	Set of sample scenarios and $ W $ is the sample size
w_l	A scenario, $w_l \in W$
y_l	Binary variable. $y_l = 1$ if current solution is infeasible in scenario $w_l \in W$, otherwise $y_l = 0$
Objective	
$\sum_{i \in A} \sum_{k \in O} \omega_i \cdot x_{ik}$	The entire observation profit for deterministic scheduling problem
f	The entire observation profit for scheduling problem under cloud coverage uncertainty

The notations used in our model are summarized in Table I. Denote A and O as the set of targets and orbits, respectively. The required observation time is denoted as ot_i for each target $i \in A$. The observation profit for target i is defined as ω_i . For each orbit $k \in O$, we define the following parameters: memory capacity M_k , energy capacity E_k , memory consumption m_k and energy cost e_k for unit time during observation, and energy consumption e'_k for unit-time angle of attitude transformation. Binary decision variable x_{ik} is introduced to represent whether target i is scheduled to be observed on orbit k .

With higher attitude maneuverability, AEOS would typically access longer VTW for each target compared to CEOS. Therefore, it is necessary to determine the observation start time for each target. A continuous decision variable TP_{ik} within $[0, 1]$ is then introduced to determine the specific satellite observation time for target i on orbit k . For example, $TP_{ik} = 0$ means that the observation start time for target i is VTS_{ik} and when TP_{ik} equals to $1/2$, the corresponding observation starts from the middle time of $[VTS_{ik}, VTE_{ik} - ot_i]$. The relationship between TP_{ik} and OW is shown as follows.

$$OTS_{ik} = TP_{ik} \cdot (VTE_{ik} - ot_i - VTS_{ik}) + VTS_{ik} \quad (1)$$

$$OTE_{ik} = OTS_{ik} + ot_i \quad (2)$$

Set $b_{ik} = 1$ when target i is visible on orbit k , and $b_{ik} = 0$ otherwise. Time intervals $[OTS_{ik}, OTE_{ik}]$ and $[VTS_{ik}, VTE_{ik}]$ respectively denote the OW and VTW of target i on orbit k . When the satellite accomplishes an observation mission, a succession of attitude transformation process is required to observe the next target. Notice the required transition time $Trans(i, OTS_{ik}, j, OTS_{jk}, k)$ from target i to j is also related to OTS_{ik} and OTS_{jk} . We denote the transition time as $Trans(i, j, k)$ for simplicity afterwards. Besides, in practical satellite application, a certain period to stabilize the satellite attitude is inevitable. Following [1], the attitude stabilization time is considered as follows.

$$Trans(i, j, k) = \max(|\theta_{ik}^{Pitch} - \theta_{jk}^{Pitch}|/s_k^{Pitch}, |\theta_{ik}^{Roll} - \theta_{jk}^{Roll}|/s_k^{Roll}) + \begin{cases} 5 & \Delta g \leq 15 \\ 10 & 15 < \Delta g \leq 40 \\ 15 & 40 < \Delta g \leq 60 \end{cases} \quad (3)$$

where Δg indicates the total angle change between two adjacent targets, s_k^{Pitch} and s_k^{Roll} represent the attitude maneuvering angle velocity of pitch and roll axes, respectively. During the observation of target i , the observation angles of AEOS are denoted as θ_{ik}^{Pitch} and θ_{ik}^{Roll} . The attitude transformation process of AEOS from target i to j also consumes energy, which is described as

$$se_{ij}^k = (|\theta_{ik}^{Pitch} - \theta_{jk}^{Pitch}| + |\theta_{ik}^{Roll} - \theta_{jk}^{Roll}|) \cdot e'_k \quad (4)$$

With the parameters defined in Equations (1)–(4), the mathematical model of multi-AEOS scheduling problem is constructed as

$$\max \sum_{i \in A} \sum_{k \in O} \omega_i \cdot x_{ik} \quad (5)$$

subject to

$$\sum_{k \in O} x_{ik} \leq 1 \quad \forall i \in A \quad (6)$$

$$x_{ik} \leq b_{ik} \quad \forall i \in A, k \in O \quad (7)$$

$$\sum_{i \in A} x_{ik} \cdot ot_i \cdot m_k \leq M_k \quad \forall k \in O \quad (8)$$

$$\sum_{i \in A} x_{ik} (se_{ij}^k + ot_i \cdot e'_k) \leq E_k \quad (9)$$

$$j \text{ is the successor target of } i \text{ on orbit } k, \quad \forall k \in O$$

$$\{x_{ik} + x_{jk} \leq 1 \mid \text{if } i \text{ is the precursor target of } j \text{ on orbit } k \text{ and} \quad (10)$$

$$g(TP_{ik}, i, TP_{jk}, j, k) > 0\} \quad \forall i, j \in A, k \in O$$

$$x_{ik} \in \{0, 1\} \quad \forall i \in A, k \in O \quad (11)$$

The objective function (5) aims to maximize the entire observation profit. Constraints (6) and (7) represent that each target cannot be observed more than once and should be arranged on available orbits. Memory constraints (8) ensure that the memory consumption for observation missions cannot exceed the memory capacity on each orbit. Constraints (9) indicate that the sum of energy consumption from satellite maneuvering and imaging should be less than or equal to the energy capacity on each orbit. The attitude transformation constraints are described in (10), where i is the precursor target of j on orbit k . Formula $g(TP_{ik}, i, TP_{jk}, j, k) > 0$ indicates that the observation ending time of target i plus the attitude transformation time from target i to j is greater than the observation start time of target j . In line with Eqs. (1) and (2), $g(TP_{ik}, i, TP_{jk}, j, k)$ is formulated as

$$\begin{aligned} g(TP_{ik}, i, TP_{jk}, j, k) &= OTE_{ik} + Trans(i, j, k) - OTS_{jk} \\ &= TP_{ik} \cdot (VTE_{ik} - ot_i - VTS_{ik}) + VTS_{ik} + ot_i + Trans(i, j, k) \\ &\quad - TP_{jk} \cdot (VTE_{jk} - ot_j - VTS_{jk}) - VTS_{jk} \end{aligned} \quad (12)$$

where TP_{ik} and TP_{jk} are independent variables. If the conditions hold, targets i and j cannot be observed on the same orbit k .

B. AEOS scheduling under uncertainty

We address modeling the cloud coverage uncertainty for AEOS scheduling in this subsection, and several necessary assumptions are considered as follows.

- 1) Cloud coverage for targets is simplified to two conditions: complete cloud occlusion and no cloud occlusion.
- 2) For each VTW, cloud occlusion or not is a random event with certain probability.
- 3) The probability of cloud coverage during the VTW is supposed to be the same.

Binary stochastic parameters λ_{ik} are defined to depict whether there is cloud coverage or not. The probability that target i can be successfully observed from orbit k is set as p_{ik} , which is randomly generated for each target. For each λ_{ik} , it will be randomly set as 1 with the probability of p_{ik} , and 0 otherwise. Subsequently, we extend the previous deterministic model to a CCP model, in which $1 - \alpha$ represents the

predefined confidence interval [44]. The objective function (5) is modified and chance constraints are added:

$$\max f \quad (13)$$

subject to

$$P \left\{ \sum_{i \in A} \sum_{k \in O} \omega_i \cdot \lambda_{ik} \cdot x_{ik} \geq f \right\} \geq 1 - \alpha \quad (14)$$

The new objective function (13) is to maximize the entire observation profit under predefined confidence interval $1 - \alpha$. The chance constraint (14) restricts the value of f . Then the CCP model for multi-AEOS scheduling with cloud coverage uncertainty is formulated as: $\max f$, subject to constraints (6)–(11) and (14).

This developed model of multiple AEOSs scheduling problem under cloud coverage uncertainty has several main characteristics and solving difficulties. First, through the adjustment of the pitch axis, AEOSs could access longer VTW for each target than CEOSs, which brings new challenges to determine the observation start time. Second, the AEOSs scheduling problem under cloud coverage uncertainty will be more difficult to solve owing to the unfixed mission execution sequence [38]. Third, as the number of observation targets increases, the scheduling complexity significantly goes up as well, calling for better scheduling heuristics. The AEOSs scheduling problem under cloud coverage uncertainty is therefore more difficult than that for non-agile satellites, due to the stronger maneuverability and more complicated calculations of attitude transformation time and energy consumption.

Besides, as far as we can see, there exists no algorithm designed specifically for our proposed model. Although there are well-designed algorithms for classic AEOSs scheduling problem (e.g., [1], [45]), introducing cloud coverage uncertainty could further increase the complexity for scheduling results evaluation, and consequently require more effective solution update process. Moreover, part of these existing algorithms do not consider energy constraints, which could also increase the problem solving difficulty. To better address the uncertain AEOSs scheduling model, designing a novel heuristic being capable of efficient solution update and handling memory and energy constraints is required.

III. SOLUTION METHOD

In this section, the sample approximation method [46] is initially introduced to calculate confidence profit considering cloud coverage uncertainty. The optimization subproblem of selecting the start time of OW is then defined and solved by the SQP method. Finally, an ISA based heuristic integrating a fast insertion algorithm is proposed to maximize the observation profit under predefined confidence interval.

A. Sample approximation method

It is difficult to calculate the probability in the chance constraint (14). Therefore, a sample approximation method is adopted to calculate observation profit approximately. Monte Carlo simulation is a numerical calculation method guided by

probability and statistics theory [47]. This statistical method generates a set of scenarios to describe situations with different cloud coverage. The scenarios can be depicted as $W = \{w_0, w_1, \dots, w_n\}$, in which any $w_l \in W$ corresponds to a group of λ_{ik} , and $|W|$ denotes the sample size.

Denote $1 - \epsilon$ as the confidence level of solution, which reflects the proportion of scenarios that satisfy the feasible solution of sample approximation problem. In line with [48], the solution which is infeasible for at most $|W| \cdot \epsilon$ scenarios can be obtained. Introduce y_l as binary variables: $y_l = 0$ if the solution is feasible for w_l and $y_l = 1$ otherwise. The sample approximation constraints are described as

$$\sum_{i \in A} \sum_{k \in O} \omega_i \cdot \lambda_{ik}^l \cdot x_{ik} \geq -y_l \cdot M + f \quad \forall w_l \in W \quad (15)$$

$$\sum_{w_l \in W} y_l \leq |W| \cdot \epsilon \quad (16)$$

In constraints (15), λ_{ik}^l denotes the value of parameter λ_{ik} under scenario w_l and M is assumed to be a large number. If $y_l = 0$, constraints (15) indicate that the total profit of observation must be larger than or equal to f . When the obtained solution is not feasible (i.e., its observation profit is less than f), the binary variable y_l will be taken as 1 for each $w_l \in W$, which ensures constraints (15) hold for the scheduling solution. Constraint (16) imposes that the number of scenarios in which the solution is infeasible should be at most $|W| \cdot \epsilon$. Therefore, to obtain a higher observation profit, the solution could be infeasible in $|W| \cdot \epsilon$ scenarios, while its observation profit in the remaining scenarios should be no less than f . The entire observation profit f under predefined confidence interval, which is the optimization function in the CCP model, now can be determined.

A lower bound of the sample size $|W|$ has been proposed in [46], and is expressed as

$$|W| \geq \frac{1}{2(\epsilon - \alpha)^2} \log\left(\frac{1}{\theta}\right) + \frac{\beta}{2(\epsilon - \alpha)^2} \log(U) \quad (17)$$

where $1 - \epsilon$ is greater than $1 - \alpha$. $1 - \theta$ is the probability when the feasible solution of the sample approximation problem simultaneously meets the original CCP model. U is set as $|X|^{1/\beta}$, where $|X|$ is the norm of the decision variables vector and β is the number of decision variables.

B. Optimization subproblem

In order to schedule more observation missions and obtain higher observation profit, the range of available time intervals between consecutive observation missions should be appropriately determined. To achieve this, the concept of time slack from [1] is introduced to describe the time intervals, and the observation start time is consequently determined by the SQP method.

1) *Definition of time slacks*: Time slacks denote the time interval between two adjacent targets on the same orbit, so the subscript k is omitted here.

As shown in Fig. 2, we intend to insert target i between its precursor target i_p and successor target i_s for better scheduling

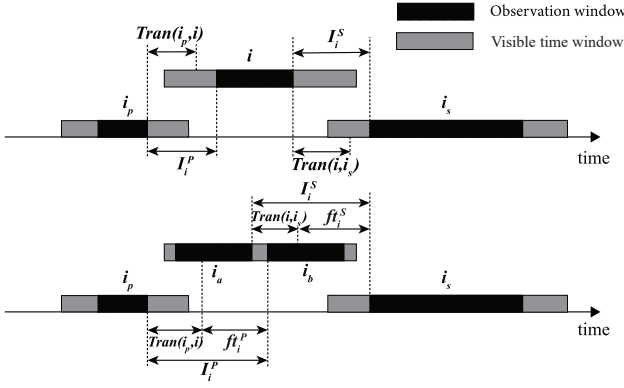


Fig. 2. Calculation diagram of the time slack.

results. The i_a and i_b are the example insertion targets in two different situations, corresponding to the time slacks for the successor and precursor targets respectively. Two time slacks are denoted as ft_i^S and ft_i^P . During the insertion process, where the time slack is utilized, the observation start times of successor and precursor targets of i are known. The value of $Trans(i, i_s)$ thus varies with OTS_i , and ft_i^S denotes the time slack between targets i and i_s , which is defined as

$$ft_i^S = \max(I_i^S - Trans(i, i_s)) \quad (18)$$

where I_i^S is the time interval from i to i_s and

$$I_i^S = OTS_i^S - OTE_i \quad (19)$$

where OTS_i^S represents the observation start time of target i_s . The independent variable of Equation (18) is OTS_i , which varies in the range of $[VTS_i, VTE_i - ot_i]$.

Substituting (1) and (2) into (19), I_i^S is expressed as

$$I_i^S = OTS_i^S - [TP_i \cdot (VTE_i - ot_i - VTS_i) + VTS_i + ot_i] \quad (20)$$

If target i is the last observation target on the orbit, then

$$\begin{aligned} ft_i^S &= VTE_i - ot_i - OTS_i \\ &= (1 - TP_i) \cdot (VTE_i - ot_i - VTS_i) \end{aligned} \quad (21)$$

Therefore ft_i^S is the function of decision variable TP_i , which suggests that the time slack is determined by the start time of OW.

The time slack between target i and its precursor target i_p , denoted as ft_i^P , can be calculated similarly. If target i is not the first target on current orbit, then

$$ft_i^P = \max(I_i^P - Trans(i_p, i)) \quad (22)$$

where I_i^P is calculated as

$$\begin{aligned} I_i^P &= OTS_i - OTE_i^P = [TP_i \cdot (VTE_i - ot_i - VTS_i) \\ &\quad + VTS_i] - OTE_i^P \end{aligned} \quad (23)$$

where OTE_i^P denotes the observation ending time of target i_p .

If target i is the first target on the orbit, then

$$ft_i^P = OTS_i - VTS_i = TP_i \cdot (VTE_i - ot_i - VTS_i) \quad (24)$$

2) *Determining the start time of OW*: To determine the start time of OW, namely the proper insertion position of the target, the optimization subproblem is constructed as follows.

$$\min (TP_i - 1/2)^2 \quad (25)$$

subject to

$$I_i^S - Trans(i, i_s) \geq 0 \quad (26)$$

$$I_i^P - Trans(i_p, i) \geq 0 \quad (27)$$

$$0 \leq TP_i \leq 1 \quad (28)$$

The objective function (25) makes TP_i as close to $1/2$ as possible. Constraints (26) and (27) represent the attitude transformation time constraints when target i has the precursor and successor targets. During the process of determining the observation start time of target i , which is critical to the insertion strategy, the OWs for the precursor and successor targets are known. According to the definitions of time interval and attitude transformation time, the unique independent parameter of the optimization subproblem is TP_i . The optimization model has the following advantages: (1) When the value of TP_i is around $1/2$, the satellite would execute observation missions above the target i , which ensures higher observation resolution. (2) The Euclidean distance [49] between TP_i and $1/2$ is adopted to ensure that the objective function is convex and thus efficient algorithms can be applied.

The optimization subproblem is established on the purpose of observing more targets and obtaining higher observation profit. Meanwhile, it is desirable to obtain high-resolution images, although we do not consider the observation imaging quality as our objective function. The suitable insertion position can be determined by solving the above quadratic optimization model and the actual observation time window is obtained simultaneously. The SQP method, which performs well in solving nonlinearly constrained optimization problems [50], is employed to solve this optimization subproblem.

C. ISA based heuristic

The design of heuristic rules is of great importance for the effectiveness and efficiency of the proposed algorithm. With effective heuristic rules, we start with an initial solution and gradually approach the solution via ISA combining with a fast insertion algorithm.

1) *Selection rules of targets and resources*: Before operating the fast insertion algorithm, the observation target and corresponding resource should be selected. The urgency for each target $Need_i$ is defined as follows.

$$Need_i = \frac{\omega_i}{\omega_{max}} + \left(1 - \frac{\sum_{k \in O} p_{ik}}{N_i} \right) \quad (29)$$

where ω_{max} represents the largest observation profit of a single target among all the observation targets and N_i denotes the number of VTWs of target i .

As seen in the definition of $Need_i$, the first item stands for the potential normalized observation profit, while the second item indicates the successful observation probability of target

i . Therefore the higher value of $Need_i$ corresponds to higher observation priority for target i .

The corresponding observation resource for the target is determined on the basis of the resource selection rule. Considering that the targets could be observed on the same orbit k , the OWs of different targets may overlap and the energy/memory consumption may exceed the orbit capacity. For each target i on orbit k , the degree of resource conflict denoted as CF_{ik} is then defined as

$$CF_{ik} = (1 - p_{ik}) \cdot \left(\frac{CFS_{ik}}{|VTW_{ik}|} + \sum_{r=1}^R \frac{Cost_{irk}}{Cap_{rk}} \right) \quad (30)$$

where CFS_{ik} denotes the length of overlapping intervals between target i and other targets on orbit k . The duration of VTW for target i on orbit k is denoted as $|VTW_{ik}|$ and R is the number of resource constraint ($R = 2$ in this work since the energy and memory constraints are considered). The consumption of resource r for target i on orbit k is represented as $Cost_{irk}$, and the remaining amount of resource r is denoted as Cap_{rk} . In Equation (30), parameter p_{ik} indicates the probability that target i will be successfully observed on orbit k . A larger p_{ik} means that target i is more likely to observe successfully. Then CF_{ik} will be lower, which means that the corresponding resource will be allocated to the target earlier. The second part $\frac{CFS_{ik}}{|VTW_{ik}|}$ represents the proportion of the VTW of target i that overlaps with other VTWs on orbit k . The third part, $\sum_{r=1}^R \frac{Cost_{irk}}{Cap_{rk}}$, represents the proportion of the resource consumed by observing the target in the remaining resource. The larger values of these two parts, the later the observation of corresponding targets will be considered and scheduled. When $Cost_{irk}$ is larger than Cap_{rk} , the target i will not be arranged to observe with the current satellite orbit. Simultaneously, this criterion also guarantees the energy constraints and memory constraints.

2) *Fast insertion algorithm*: Suppose that target i is to be executed on orbit k , and there are already two scheduled targets, the successor target $i+1$ and the precursor target $i-1$, on the same orbit. The fast insertion algorithm is then invoked to insert target i between the two scheduled targets. The main procedure of the fast insertion algorithm is summarized in Fig. 3, and the detailed procedure is described as follows.

Step 1: During the initialization process, TP_{ik} is set as $1/2$, and the parameters I_i^P , I_i^S , $Trans(i_p, i)$ and $Trans(i, i_s)$ are calculated. Then we check the constraints (8)–(11) to determine x_{ik} .

Step 2: If the initial OW for target i (denoted as OW_i) does not satisfy the transition time constraint, shuffle OW_i within the VTW of target i on orbit k in order to search a proper position that meets the constraint. Through solving the optimization subproblem defined in Section III-B, the value of TP_{ik} corresponding to the position of OW_i is updated if constraints (26) and (27) are simultaneously satisfied, then go to Step 7. Otherwise, go to Step 3.

Step 3: Fix OW_i at the initial position, namely the value of TP_{ik} equals to $1/2$, and calculate the subsequent time slack of OW_{i+1} and the precursor time slack of OW_{i-1} , which are de-

noted as ft_{i+1}^S and ft_{i-1}^P , respectively. If constraint (27) holds, move forward OW_{i+1} and go to Step 4. If constraint (26) holds, move backward OW_{i-1} and go to Step 5. If none of them holds, go to Step 6.

Step 4: If condition $ft_{i+1}^S \geq I_i^S - Trans(i, i+1)$ holds, move forward the successor observation time window OW_{i+1} . If OW_i can be inserted successfully, go to Step 7. Otherwise, current insertion fails and the algorithm ends.

Step 5: If condition $ft_{i-1}^P \geq I_i^P - Trans(i-1, i)$ holds, move backward the precursor observation time window OW_{i-1} . If OW_i can not be inserted, end the current insertion procedure. Otherwise, go to Step 7.

Step 6: If conditions $ft_{i+1}^S \geq I_i^S - Trans(i, i+1)$ and $ft_{i-1}^P \geq I_i^P - Trans(i-1, i)$ hold simultaneously, insert OW_i by moving the two adjacent OWs at the same time (Repeat Step 4 and Step 5). If the above conditions hold, go to Step 7. Otherwise, end current insertion process.

Step 7: Once OW_i has been inserted successfully, update the information of resource consumption on orbit k .

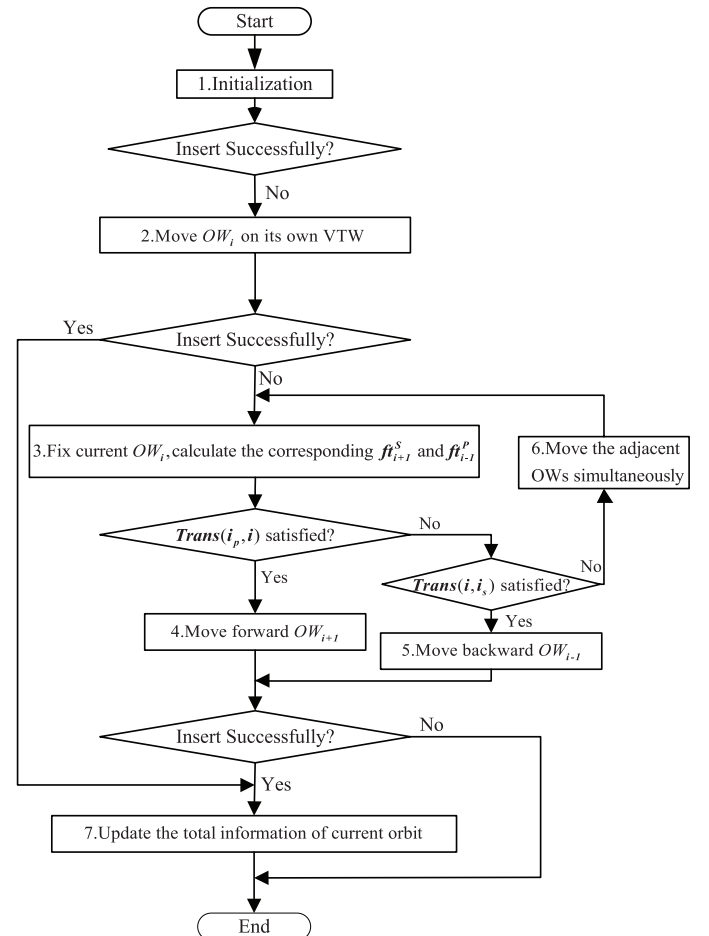


Fig. 3. The flow chart of the fast insertion algorithm.

3) *Structure of the ISA based heuristic*: Metaheuristic algorithms have been extensively employed in various practical engineering problems [51], [52], [53]. Particularly, the simulated annealing algorithm proposed decades ago [54], [55], is a stochastic optimization method. Possessing the ability to

acquire near-optimal solutions within an acceptable time, simulated annealing has been widely applied in the combinatorial optimization problems. Combining the fast insertion strategy, we develop an ISA based heuristic for multi-AEOS scheduling under cloud coverage uncertainty. The primary structure of ISA based heuristic is shown in Fig. 4, where each step is described as follows.

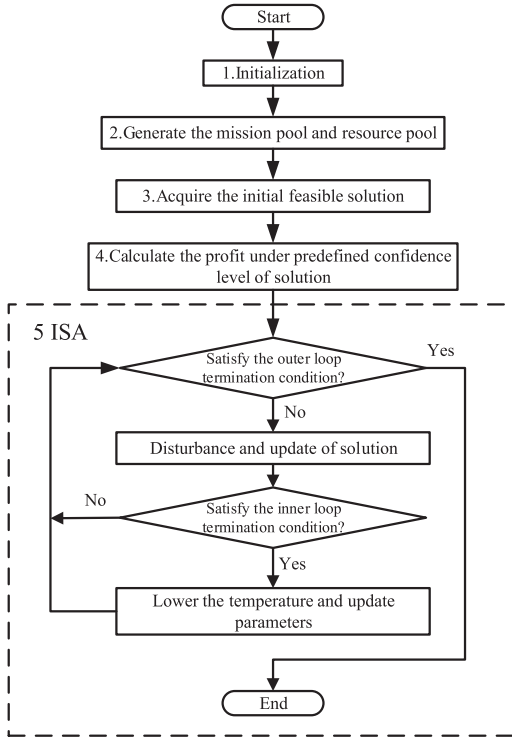


Fig. 4. The structure of ISA based heuristic.

Step 1: Initialize all input parameters, such as satellite orbital elements, the information of targets and the VTWs. Besides, obtain an initial scheduling result using the proposed selection rules of targets and resources in Section III-C1.

Step 2: Calculate $Need_i$ and CF_{ik} for each target i on available orbit k . By sorting these two factors in order, generate the initial mission pool and resource pool.

Step 3: Generate initial feasible solution. Select targets to be observed from the mission pool and corresponding available resources in order. The resource with lower degree of conflict has higher priority. If the target is successfully scheduled, delete related target and resource in the pools.

Step 4: Calculate confidence observation profit via the sample approximation method for the initial solution.

Step 5: The dotted box contains the general procedure of ISA, which is detailed in Algorithm 1. The input parameters of ISA are given initially, where higher γ means larger disturbance of current solution, minor ζ_m indicates lower increasing speed of nF , which denotes the unaccepted numbers of new solution. nF_m^T is the upper limit of the iterations number in inner loop, while nF_m and $nIter_m$ are set as the maximum numbers of iterations in outer loop.

During each iteration, a certain number of targets would be deleted and a new solution is generated with randomly selecting targets from the mission pool and invoking the fast insertion algorithms. Using the popular Metropolis method [54], the acceptance probability P_a is designed as

$$P_a = \begin{cases} 1 & \Delta f \geq 0 \\ e^{\Delta f/T} & \Delta f < 0 \end{cases} \quad (31)$$

where $\Delta f = f^{new} - f$. With the help of Metropolis strategy, ISA can jump out of local optima to some extent. Subsequently, a updating strategy for nF^T is proposed:

$$nF^T = \begin{cases} 0 & \zeta \geq \zeta_m \\ nF^T + 1 & \zeta < \zeta_m \end{cases} \quad (32)$$

where T is a mark of the current temperature, which does not participate in calculations, and ζ indicates the improving ratio of the new solution compared to the old one, calculated as

$$\zeta = (f^{new} - f)/f \quad (33)$$

When the inner loop ends, current temperature would decrease due to $\alpha_T < 1$. Conversely, a longer length of Markov chain is updated by $\alpha_L > 1$. Finally, we output the best scheduling solution S_{best} and corresponding observation profit f_{best} . The complexity of the proposed algorithm has been evaluated in Table II, indicating the total time computational complexity is $O(n^2)$, where n denotes the number of targets.

Algorithm 1 Procedure of ISA

Input:

Information of initial profit f_0 and number of visible targets $vTar$, initial scheduling scheme S_0 and the number of targets arranged $aTar^0$, parameters of ISA: $\zeta_m, \gamma, \alpha_T, \alpha_L, T_0, nF_m, nF_m^T$ and $nIter_m$

Output:

The best total profit f_{best} and corresponding scheduling scheme S_{best}

- 1: Initialization: $aTar^T \leftarrow aTar^0, T \leftarrow T_0, L^T \leftarrow vTar/2, f \leftarrow f_0, f_{best} \leftarrow f_0, S \leftarrow S_0, S_{best} \leftarrow S_0$;
- 2: **while** $nF < nF_m$ or $nIter < nIter_m$ **do**
- 3: **while** $nF^T < nF_m^T$ or $nIter^T < L^T$ **do**
- 4: Delete $\gamma \times aTar^T$ targets from current solution randomly and generate a new scheduling scheme S^{new} including $f^{new}, aTar^{new}$;
- 5: Generate a uniform random number u in $[0,1]$
- 6: **if** $u < P_a$ **then**
- 7: $f \leftarrow f^{new}, S \leftarrow S^{new}, aTar^T \leftarrow aTar^{new}$
- 8: update nF^T according to (32)
- 9: **if** $f > f_{best}$ **then**
- 10: $f_{best} \leftarrow f, S_{best} \leftarrow S$
- 11: **end if**
- 12: **else**
- 13: $nF^T \leftarrow nF^T + 1$
- 14: **end if**
- 15: $nIter^T \leftarrow nIter^T + 1$
- 16: **end while**
- 17: $nF \leftarrow nF + nF^T$
- 18: $nIter \leftarrow nIter + nIter^T$
- 19: $T \leftarrow T \times \alpha_T, L^T \leftarrow L^T \times \alpha_L$
- 20: $nF^T = 0, nIter^T = 0$
- 21: **end while**
- 22: Output f_{best} and S_{best}

IV. COMPUTATIONAL EXPERIMENTS

A. Data generation

The experiments are conducted using Intel (R) Core (TM) i7-4790K CPU at 4.00 GHz and 12.0 GB of RAM on Windows

TABLE II
THE COMPLEXITY OF THE PROPOSED ALGORITHM.

Procedure of Algorithm	Complexity
Initialization	$O(1)$
Generate the mission pool and resource pool	$O(n)$
Acquire the initial feasible solution	$O(n^2)$
Calculate the profit under predefined confidence level of solution	$O(n^2)$
Disturbance and update of solution	$O(n^2)$
Lower the temperature and update parameters	$O(1)$

10 64-bits OS. The ISA based heuristic is coded in Matlab and the scheduling scenarios are generated as follows. Without benchmark dataset for uncertain AEOSs scheduling problems, we design several instances in line with [1], [5], [56]. The targets are generated according to a random distribution over the world and several specific interest areas. The total number of observation targets is 500, 650, 800 or 950, with a worldwide distribution of 500 targets and additionally several areas with 150 targets each. The profit ω_i of each target $i \in A$ is uniformly distributed from 1 to 10. The worldwide distribution targets locate in the range of latitude between 60° S- 60° N and longitude between 180° W- 180° E. Several interest regions are predefined mainly in China (3° N- 53° N and 74° E- 133° E), Australia (43° S- 10° S and 112° E- 154° E), and America (24° N- 49° N and 73° W- 125° W), among which one, two or three regions are selected for different scenarios. The constraint that the solar altitude angle for each observation is not less than 0° is also taken into consideration in generating VTWs.

The mission horizon is set as 24 hours, starting from 2017/01/01 00:00:00. The orbital parameters of satellites in the scenarios are shown in Table III. The first column *ID* denotes the name of satellite, and the other columns indicate the length of semi-major axis (*a*), eccentricity (*e*), inclination (*i*), right ascension of the ascending node (Ω), argument of perigee (ω) and mean anomaly (*M*), respectively. The satellites are designed with the largest pitch degree of 30° and roll degree of 30° , where the angular velocity are all set as $3^\circ/s$. The unit-time memory consumption of imaging m_k is 100 MB/s, while the energy consumption of unit-time imaging and unit-angle maneuvering are 500 and 1000 *W*, respectively. In line with [38], the parameters of the CCP are fixed as $1 - \alpha = 0.90$, $1 - \epsilon = 0.99$ and $1 - \theta = 0.99$. The value of $|W|$ will be set as the integer lower bound determined by Equation (17). The default parameters of ISA are set as $\alpha_T = 0.95$, $\alpha_L = 1.05$, $\zeta_m = 0.05$, $T_0 = 1000$, $nF_m^T = 50$ and $nIter_m = 2000$.

TABLE III
ORBITAL PARAMETERS OF THE SATELLITES.

<i>ID</i>	<i>a</i> (km)	<i>e</i>	<i>i</i> ($^\circ$)	Ω ($^\circ$)	ω ($^\circ$)	<i>M</i> ($^\circ$)
Sat1	6903.673	0.001655	97.5839	97.8446	50.5083	2.0288
Sat2	6903.730	0.001558	97.5310	95.1761	52.2620	31.4501
Sat3	6909.065	0.000997	97.5840	93.1999	254.4613	155.2256
Sat4	6898.602	0.001460	97.5825	92.3563	276.7332	140.1878

B. Computational results

1) *Parameters setting*: In the proposed algorithm, two parameters of the disturbance rate γ and the maximum iteration

number nF_m play important roles in the acquisition of better results. The disturbance rate γ for arranged targets would affect the scheduling variation range, and nF_m controls the termination condition. The tuning experiments for γ and nF_m have been conducted where the energy and memory capacity on each orbit are set as $E_m = 80$ kJ and $M_m = 7500$ MB.

The simulation results for different scenarios ($n = 500, 650, 800, 950$) are shown in Fig. 5. The green triangle symbol and the orange horizontal line indicate the average and median of the observation profit of 10 runs, respectively. The box plot shows the distribution of the results and the purple square dots represent the algorithm running time. As the number of observation targets increases, the observation profit under each set of parameters improves gradually, while the program running time also has an ascending trend. Compared to the instance with $\gamma = 0.10$ and $nF_m = 100$, the observation profit of other groups does not have generally evident increase and even slightly decrease, while the program running time has improved significantly in all scenarios with different number of targets. In order to strike a balance between the performance and efficiency of the algorithm, the set of parameters $\gamma = 0.10$ and $nF_m = 100$ is therefore selected for the following experiments in multiple AEOSs scheduling problem with cloud coverage uncertainty.

2) *Constraint testing*: The energy and memory constraints are crucial for multi-AEOS scheduling with uncertainty problem. We test the constraints with different parameters and report the simulation results in Fig. 6. As shown in the four subplots, the observation profit clearly increases with more number of targets. When E_m is fixed, the observation profit improves with the increase of M_m . Similarly, for the instances with the same M_m , the profit also goes up as E_m increases, indicating the influence of the constraints for the multi-AEOS scheduling problem.

For the scenario with 500 targets whose results are shown in the top left subplot, the most significant profit improvement appears when E_m varies from 40 to 80 kJ, and the average increase of mean observation profit in conditions of different memory capacity ($M_m = 5000, 7500$ and 10000 MB) is about 150. When E_m is set as 120 kJ or 160 kJ, we observe that the observation profit increases slowly, indicating that the energy capacity with 80 kJ on each orbit may be large enough for scheduling in this scenario.

When the energy constraint is not binding anymore for the AEOSs scheduling, the memory capacity would be the most important factor for the scheduling result. It can be observed from the two subplots below. For the scenarios with E_m setting as 120 and 160 kJ, the observation profit dramatically increases with the increase of the memory capacity. This is because that the energy is sufficient for observation and the memory storage is not enough in current situations. In conclusion, the energy and memory constraints have a huge impact on the observation profit, and the problem can be effectively solved by the proposed heuristic.

3) *Comparison experiments with other heuristics*: To verify the effectiveness of the proposed algorithm, one should compare it with existing algorithms. However, as mentioned in the introduction, no existing algorithms can be readily applied to

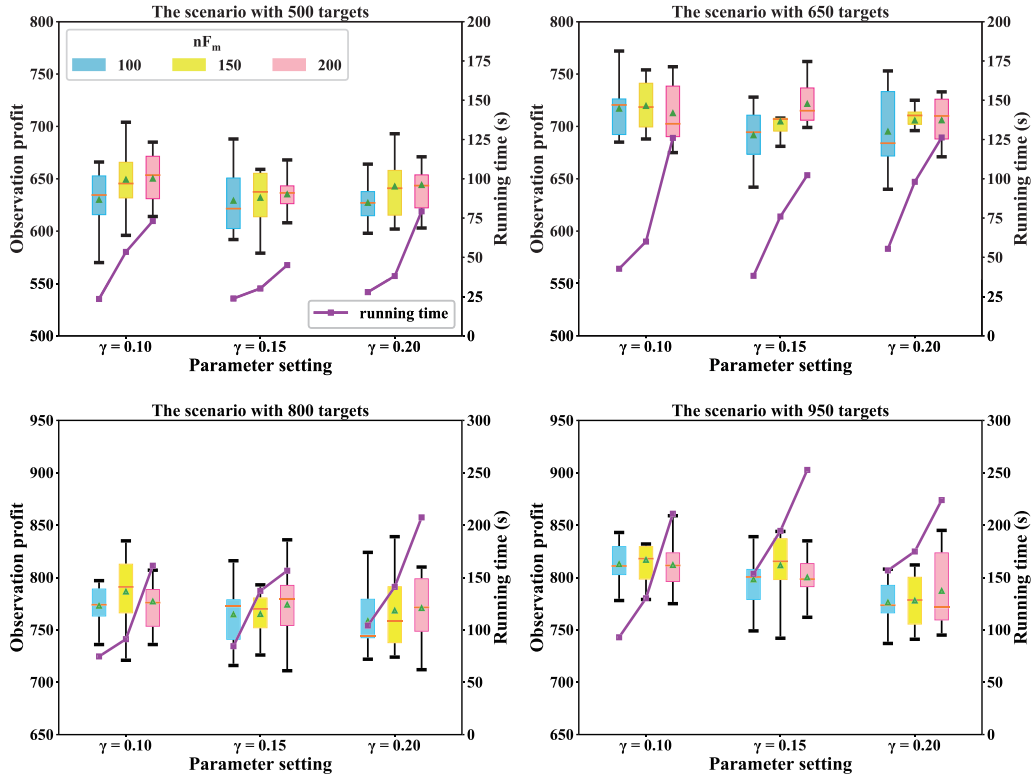


Fig. 5. Simulation results of parameter setting with different number of targets.

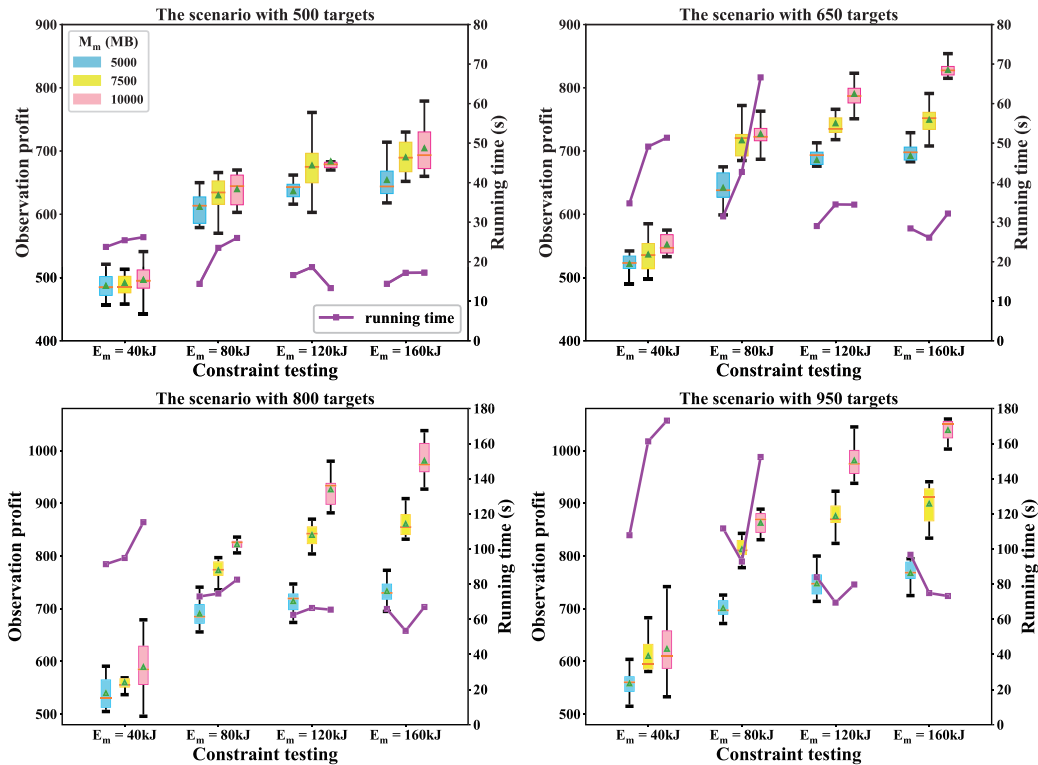


Fig. 6. Simulation results of constraint testing with different number of targets.

the multiple AEOSs scheduling problem under cloud coverage uncertainty. Therefore we introduce the genetic algorithm (GA), the adaptive large neighborhood search (ALNS) algorithm proposed in [1], the bidirectional dynamic programming based iterated local search (BDP-ILS) algorithm presented in [45], and modify them for comparisons. The original observation profit in ALNS is redefined as the profit under certain confidence level, and for fair comparison, the maximum iteration number of ALNS is changed to 100 and 500 (denoted as ALNS-100 and ALNS-500, respectively), remaining other parameters the same as in [1]. Apart from the adjustment of the uncertain profit, the memory constraint is evaluated during the target insertion and the energy consumption has been calculated for each solution in the BDP-ILS algorithm. Moreover, in order to ensure comparable algorithm run time with ISA, the iteration number and the removal ratio of BDP-ILS are determined as 100 and 0.1, respectively. A similar process with the ISA is applied in the GA, by initializing the scheduling results with the fast insertion algorithm and executing crossover and mutation rules during each iteration. According to preliminary experiments, the parameters of GA are determined as follows.

- Population size: 10
- Crossover probability of population individual: 0.5
- Crossover and mutation criterion: single point
- Iteration: 100

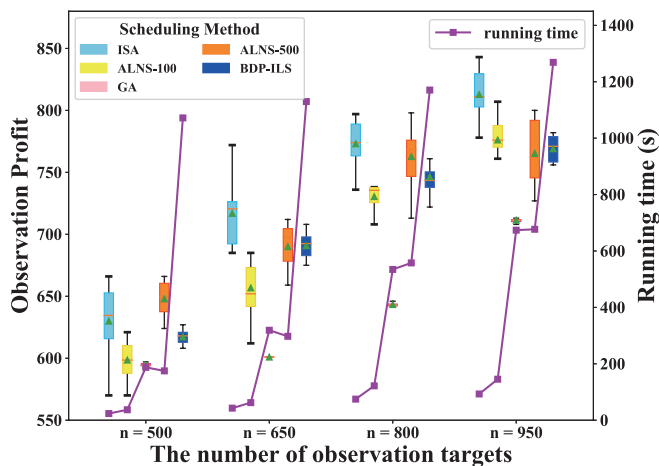


Fig. 7. Comparison experiments results with different algorithms.

The results of the comparative experiments are shown in Fig. 7, in which the green triangle symbol and the orange horizontal line indicate the average and median values of the observation profit of 10 runs, respectively. The box plot shows the distribution of the results and the purple square dots represent the algorithm running time. As can be seen from Fig. 7, the mean observation profit of each scenario obtained by ISA is higher than that of ALNS-100, GA and BDP-ILS, while the program running time of ISA is the shortest. Although GA consumes a longer computation time, the scheduling profit is worse than the results of ISA and ALNS-100/500. This is because the crossover and mutation strategies contribute little to the generation of high-quality scheduling schemes, resulting

in stable solutions. The ALNS algorithm will exit the loop immediately when all targets are arranged for observation, which is efficient for deterministic AEOS scheduling while not the case for uncertain scheduling. ISA and ALNS-500 have close performance in terms of the observation profit. Specifically, ALNS-500 is fractionally superior to ISA in the scenario with 500 targets, while ISA performs better in the scenarios with more observation targets. Meanwhile, ALNS-500 takes a longer computational time than ISA. BDP-ILS consumes the longest computation time because the observation start time has to be iteratively calculated for energy constraints evaluation. Relying on the fast insertion algorithm combined with a strategy to determine the observation start time, ISA can obtain scheduling results with high efficiency. Overall, these results suggest that ISA outperforms ALNS, GA and BDP-ILS, which verifies the effectiveness of the proposed algorithm.

4) *Sensitivity analysis*: The confidence interval and the confidence level of the sample approximation method may impact the results of the observation profit and program running time. To test the influence of these factors, we adjust $1 - \alpha$ with 0.90, 0.85 and 0.80, $1 - \epsilon$ with 0.99, 0.95, 0.90 and 0.85. Notice that $1 - \epsilon > 1 - \alpha$ should be maintained in line with the sample approximation method. E_m and M_m are fixed as 80 kJ and 7500 MB. For each combination of α and ϵ in scenarios with 500, 650, 800 or 950 targets, 10 runs are conducted. Therefore we entirely have $9 \times 4 \times 10 = 360$ runs to analyze the sensitivity of the ISA based heuristic.

The simulation results of different parameter combinations are reported in Fig. 8. Notably, parameter ϵ has a significant impact on the performance of the proposed algorithm. It is apparent from each subplot in Fig. 8 that the observation profit improves with the increase of ϵ . Theoretically, a larger value of ϵ means a lower confidence level, resulting in the acceptance of a less conservative solution, which complies with the simulation results. In summary, the ISA based heuristic overall performs well in different settings of the confidence level of the sample approximation method, indicating the broad feasibility of the proposed algorithm.

V. CONCLUSIONS

The multiple AEOSs scheduling problem under cloud coverage uncertainty is addressed in this work. We aim to maximize the total observation profit under a predefined confidence level. The constraint satisfaction model is constructed, where the energy & memory constraints and attitude maneuverability constraint are taken into consideration. The CCP method is further introduced to describe the cloud coverage uncertainty. However, it is difficult to calculate the observation profit in the CCP model. The sample approximation method is then adopted to reformulate the chance constraint and calculate the target profit, where the feasibility is guaranteed within a predefined confidence level. Subsequently, the optimization subproblem based on the concept of time slack is defined to determine the observation start time. Finally, the ISA based heuristic based upon the fast insertion algorithm is developed to iteratively optimize observation profit under cloud coverage uncertainty. Computational results show that the ISA

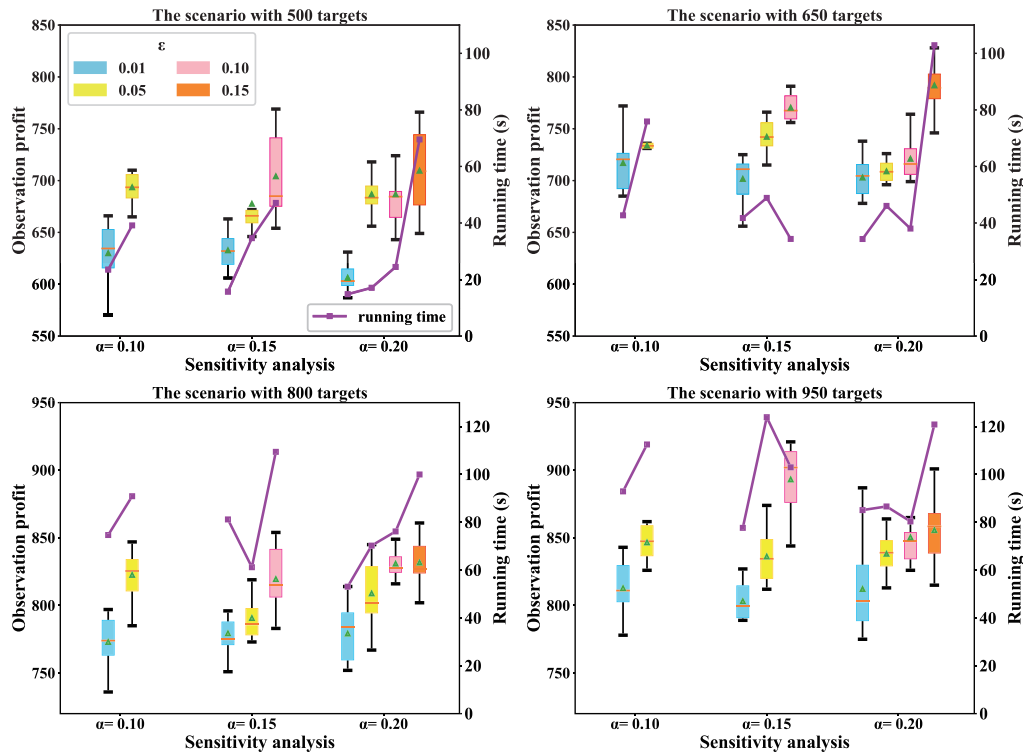


Fig. 8. Simulation results of sensitivity analysis with different number of targets.

based heuristic could efficiently obtains solution for multi-AEOS scheduling with cloud coverage uncertainty. Compared to ALNS, GA and BDP-ILS in AEOSs scheduling under cloud coverage uncertainty, the proposed heuristic could obtain better scheduling results utilizing a shorter time, which verifies the efficiency and effectiveness of our algorithm.

Future research on AEOSs scheduling considering cloud coverage uncertainty may be oriented in two directions. The objective function in this study is to maximize the total confidence observation profit, while the observation angle of AEOS could also affect the observation missions. Therefore, multi-objective optimization method could be taken into consideration. In addition, the onboard autonomous scheduling for multiple AEOSs is more practical in dealing with various uncertainties. This asserts a high claim for real-time scheduling, which deserves to be further studied.

ACKNOWLEDGMENT

Our deepest gratitude goes to the anonymous reviewers for their careful work and thoughtful suggestions that have improved this paper substantially. We also thank Guansheng Peng for enthusiastic discussions.

REFERENCES

- [1] X. Liu, G. Laporte, Y. Chen, and R. He, "An adaptive large neighborhood search metaheuristic for agile satellite scheduling with time-dependent transition time," *Computers & Operations Research*, vol. 86, pp. 41–53, 2017.
- [2] X. Chen, G. Reinelt, G. Dai, and A. Spitz, "A mixed integer linear programming model for multi-satellite scheduling," *European Journal of Operational Research*, vol. 275, no. 2, pp. 694–707, 2019.
- [3] X. Wang, C. Han, P. Yang, and X. Sun, "Onboard satellite visibility prediction using metamodeling based framework," *Aerospace Science and Technology*, vol. 94, p. 105377, 2019.
- [4] Y. Gu, C. Han, and X. Wang, "A kriging based framework for rapid satellite-to-site visibility determination," in *2019 IEEE 10th International Conference on Mechanical and Aerospace Engineering (ICMAE)*. IEEE, 2019, pp. 262–267.
- [5] L. He, X. Liu, G. Laporte, Y. Chen, and Y. Chen, "An improved adaptive large neighborhood search algorithm for multiple agile satellites scheduling," *Computers & Operations Research*, vol. 100, pp. 12–25, 2018.
- [6] M. Lemaître, G. Verfaillie, F. Jouhaud, J.-M. Lachiver, and N. Bataille, "Selecting and scheduling observations of agile satellites," *Aerospace Science and Technology*, vol. 6, no. 5, pp. 367–381, 2002.
- [7] V. Gabrel, A. Moulet, C. Murat, and V. T. Paschos, "A new single model and derived algorithms for the satellite shot planning problem using graph theory concepts," *Annals of Operations Research*, vol. 69, pp. 115–134, 1997.
- [8] V. Gabrel and D. Vanderpooten, "Enumeration and interactive selection of efficient paths in a multiple criteria graph for scheduling an Earth observing satellite," *European Journal of Operational Research*, vol. 139, no. 3, pp. 533–542, 2002.
- [9] W. J. Wolfe and S. E. Sorensen, "Three scheduling algorithms applied to the Earth observing systems domain," *Management Science*, vol. 46, no. 1, pp. 148–166, 2000.
- [10] T. Benoist and B. Rottembourg, "Upper bounds for revenue maximization in a satellite scheduling problem," *Quarterly Journal of the Belgian French & Italian Operations Research Societies*, vol. 2, no. 3, pp. 235–249, 2004.
- [11] W. C. Lin, D. Y. Liao, C. Y. Liu, and Y. Y. Lee, "Daily imaging scheduling of an Earth observation satellite," *IEEE Transactions on Systems, Man, and Cybernetics - Part A: Systems and Humans*, vol. 35, no. 2, pp. 213–223, 2005.
- [12] F. Marinelli, S. Nocella, F. Rossi, and S. Smriglio, "A lagrangian heuristic for satellite range scheduling with resource constraints," *Computers & Operations Research*, vol. 38, no. 11, pp. 1572–1583, 2011.
- [13] G. Wu, J. Liu, M. Ma, and D. Qiu, "A two-phase scheduling method with the consideration of task clustering for Earth observing satellites," *Computers & Operations Research*, vol. 40, no. 7, pp. 1884–1894, 2013.

- [14] G. Wu, W. Pedrycz, H. Li, M. Ma, and J. Liu, "Coordinated planning of heterogeneous Earth observation resources," *IEEE Transactions on Systems, Man, and Cybernetics: Systems*, vol. 46, no. 1, pp. 109–125, 2015.
- [15] G. Wu, H. Wang, W. Pedrycz, H. Li, and L. Wang, "Satellite observation scheduling with a novel adaptive simulated annealing algorithm and a dynamic task clustering strategy," *Computers & Industrial Engineering*, vol. 113, pp. 576–588, 2017.
- [16] X. Wang, R. Leus, and C. Han, "Fixed interval scheduling of multiple Earth observation satellites with multiple observations," in *2018 9th International Conference on Mechanical and Aerospace Engineering (ICMAE)*. IEEE, 2018, pp. 28–33.
- [17] X. Hu, W. Zhu, B. An, P. Jin, and W. Xia, "A branch and price algorithm for EOS constellation imaging and downloading integrated scheduling problem," *Computers & Operations Research*, vol. 104, pp. 74–89, 2019.
- [18] X. Wang, G. Wu, L. Xing, and W. Pedrycz, "Agile earth observation satellite scheduling over 20 years: formulations, methods and future directions," *IEEE Systems Journal*, 2020, doi: 10.1109/JSYST.2020.2997050.
- [19] G. Beaumet, G. Verfaillie, and M. C. Charneau, "Feasibility of autonomous decision making on board an agile Earth-observing satellite," *Computational Intelligence*, vol. 27, no. 1, pp. 123–139, 2011.
- [20] S. Liu, Y. Chen, L. Xing, and X. Guo, "Time-dependent autonomous task planning of agile imaging satellites," *Journal of Intelligent & Fuzzy Systems*, vol. 31, no. 3, pp. 1365–1375, 2016.
- [21] Y. She, S. Li, and Y. Zhao, "Onboard mission planning for agile satellite using modified mixed-integer linear programming," *Aerospace Science and Technology*, vol. 72, pp. 204–216, 2018.
- [22] X.-W. Wang, Z. Chen, and C. Han, "Scheduling for single agile satellite, redundant targets problem using complex networks theory," *Chaos, Solitons & Fractals*, vol. 83, pp. 125–132, 2016.
- [23] X. Wang, C. Han, R. Zhang, and Y. Gu, "Scheduling multiple agile earth observation satellites for oversubscribed targets using complex networks theory," *IEEE Access*, vol. 7, pp. 110605–110615, 2019.
- [24] D.-H. Cho, J.-H. Kim, H.-L. Choi, and J. Ahn, "Optimization-based scheduling method for agile Earth-observing satellite constellation," *Journal of Aerospace Information Systems*, vol. 15, no. 11, pp. 611–626, 2018.
- [25] L. Li, H. Chen, J. Li, N. Jing, and M. Emmerich, "Preference-based evolutionary many-objective optimization for agile satellite mission planning," *IEEE Access*, vol. 6, pp. 40963–40978, 2018.
- [26] B. Du, S. Li, Y. She, W. Li, H. Liao, and H. Wang, "Area targets observation mission planning of agile satellite considering the drift angle constraint," *Journal of Astronomical Telescopes, Instruments, and Systems*, vol. 4, no. 4, p. 047002, 2018.
- [27] G. Peng, G. Song, L. Xing, A. Gunawan, and P. Vansteenwegen, "An exact algorithm for agile Earth observation satellite scheduling with time-dependent profits," *Computers & Operations Research*, vol. 120, p. 104946, 2020.
- [28] J. Wang, X. Zhu, D. Qiu, and L. T. Yang, "Dynamic scheduling for emergency tasks on distributed imaging satellites with task merging," *IEEE Transactions on Parallel and Distributed Systems*, vol. 25, no. 9, pp. 2275–2285, 2014.
- [29] J. Wang, X. Zhu, L. T. Yang, J. Zhu, and M. Ma, "Towards dynamic real-time scheduling for multiple Earth observation satellites," *Journal of Computer and System Sciences*, vol. 81, no. 1, pp. 110–124, 2015.
- [30] B. Du and S. Li, "A new multi-satellite autonomous mission allocation and planning method," *Acta Astronautica*, 2018.
- [31] E. V. Ntagioui, C. Iacopino, N. Policella, R. Armellini, and A. Donati, "Ant-based mission planning: Two examples," in *2018 SpaceOps Conference*, 2018, p. 2498.
- [32] L. He, X.-L. Liu, Y.-W. Chen, L.-N. Xing, and K. Liu, "Hierarchical scheduling for real-time agile satellite task scheduling in a dynamic environment," *Advances in Space Research*, vol. 63, no. 2, pp. 897–912, 2019.
- [33] A. Globus, J. Crawford, J. Lohn, and A. Pryor, "A comparison of techniques for scheduling Earth observing satellites," in *Association for the Advancement of Artificial Intelligence*, 2004, pp. 836–843.
- [34] X. Wang, G. Song, R. Leus, and C. Han, "Robust earth observation satellite scheduling with uncertainty of cloud coverage," *IEEE Transactions on Aerospace and Electronic Systems*, 2019.
- [35] J. Ju and D. P. Roy, "The availability of cloud-free Landsat ETM+ data over the conterminous United States and globally," *Remote Sensing of Environment*, vol. 112, no. 3, pp. 1196–1211, 2008.
- [36] M. He and R. He, "Research on agile imaging satellites scheduling techniques with the consideration of cloud cover," *Sci Technol Eng*, vol. 13, no. 28, pp. 8373–8379, 2013.
- [37] D.-Y. Liao and Y.-T. Yang, "Imaging order scheduling of an Earth observation satellite," *IEEE Transactions on Systems, Man, and Cybernetics, Part C (Applications and Reviews)*, vol. 37, no. 5, pp. 794–802, 2007.
- [38] J. Wang, E. Demeulemeester, and D. Qiu, "A pure proactive scheduling algorithm for multiple Earth observation satellites under uncertainties of clouds," *Computers & Operations Research*, vol. 74, pp. 1–13, 2016.
- [39] C. G. Valicka, D. Garcia, A. Staid, J.-P. Watson, G. Hackebeil, S. Rathinam, and L. Ntaimo, "Mixed-integer programming models for optimal constellation scheduling given cloud cover uncertainty," *European Journal of Operational Research*, vol. 275, no. 2, pp. 431–445, 2019.
- [40] J. Wang, E. Demeulemeester, X. Hu, D. Qiu, and J. Liu, "Exact and heuristic scheduling algorithms for multiple Earth observation satellites under uncertainties of clouds," *IEEE Systems Journal*, pp. 1–12, 2018.
- [41] J. Wang, E. Demeulemeester, X. Hu, and G. Wu, "Expectation and SAA models and algorithms for scheduling of multiple Earth observation satellites under the impact of clouds," *IEEE Systems Journal*, 2020, doi: 10.1109/JSYST.2019.2961236.
- [42] L. He, X. Liu, L. Xing, and Y. Chen, "Cloud avoidance scheduling algorithm for agile optical satellites," *Journal of Computational and Theoretical Nanoscience*, vol. 13, no. 6, pp. 3691–3705, 2016.
- [43] E. Bensana, G. Verfaillie, C. Michelon-Edery, and N. Bataille, "Dealing with uncertainty when managing an Earth observation satellite," *European Space Agency-Publications-ESA SP*, vol. 440, pp. 205–210, 1999.
- [44] B. Liu, "Some research problems in uncertainty theory," *Journal of Uncertain Systems*, vol. 3, no. 1, pp. 3–10, 2009.
- [45] G. Peng, R. Dewil, C. Verbeeck, A. Gunawan, L. Xing, and P. Vansteenwegen, "Agile Earth observation satellite scheduling: An orienteering problem with time-dependent profits and travel times," *Computers & Operations Research*, vol. 111, pp. 84–98, 2019.
- [46] J. Luedtke and S. Ahmed, "A sample approximation approach for optimization with probabilistic constraints," *SIAM Journal on Optimization*, vol. 19, no. 2, pp. 674–699, 2008.
- [47] N. Metropolis and S. Ulam, "The monte carlo method," *Journal of the American statistical association*, vol. 44, no. 247, pp. 335–341, 1949.
- [48] A. Ruszczyński, "Probabilistic programming with discrete distributions and precedence constrained knapsack polyhedra," *Mathematical Programming*, vol. 93, no. 2, pp. 195–215, 2002.
- [49] P.-E. Danielsson, "Euclidean distance mapping," *Computer Graphics and Image Processing*, vol. 14, no. 3, pp. 227–248, 1980.
- [50] P. T. Boggs and J. W. Tolle, "Sequential quadratic programming," *Acta Numerica*, vol. 4, pp. 1–51, 1995.
- [51] R. Wang, S. Lai, G. Wu, L. Xing, L. Wang, and H. Ishibuchi, "Multi-clustering via evolutionary multi-objective optimization," *Information Sciences*, vol. 450, pp. 128–140, 2018.
- [52] J. Zhang, L. Wang, and L. Xing, "Large-scale medical examination scheduling technology based on intelligent optimization," *Journal of Combinatorial Optimization*, vol. 37, no. 1, pp. 385–404, 2019.
- [53] S. Xiang, L. Xing, L. Wang, and K. Zou, "Comprehensive learning pigeon-inspired optimization with tabu list," *Science China Information Sciences*, vol. 62, no. 7, p. 70208, 2019.
- [54] S. Kirkpatrick, C. D. Gelatt, and M. P. Vecchi, "Optimization by simulated annealing," *Science*, vol. 220, no. 4598, pp. 671–680, 1983.
- [55] S. Kirkpatrick, "Optimization by simulated annealing: Quantitative studies," *Journal of Statistical Physics*, vol. 34, no. 5-6, pp. 975–986, 1984.
- [56] C. Han, X. Wang, G. Song, and R. Leus, "Scheduling multiple agile Earth observation satellites with multiple observations," *arXiv preprint arXiv:1812.00203*, 2018.

This figure "GuPhoto.jpg" is available in "jpg" format from:

<http://arxiv.org/ps/2003.08363v2>

This figure "HanPhoto.jpg" is available in "jpg" format from:

<http://arxiv.org/ps/2003.08363v2>

This figure "WangPhoto.jpg" is available in "jpg" format from:

<http://arxiv.org/ps/2003.08363v2>

This figure "WuPhoto.jpg" is available in "jpg" format from:

<http://arxiv.org/ps/2003.08363v2>